Electronic and rotational energy relaxation in molecular helium

J.-C. Gauthier, J.-P. Geindre, J.-P. Moy, and J.-F. Delpech
Groupe d'Electronique dans les Gaz, Institut d'Electronique Fondamentale, Bât. 220, Université Paris-XI, 91405 Orsay, France
(Received 14 July 1975; revised manuscript received 28 October 1975)

We have selectively pumped the $He_2(a\,^3\Sigma_u^+, v=0, J=5) \rightarrow He_2(e\,^3\Pi_g, v=0, J=6)$ transition of molecular helium with the light produced by a pulsed dye laser, and we have subsequently followed by fluorescence measurements on a nanosecond time scale both the relaxation of the electronic excitation energy and the energy redistribution among rotational sublevels of the $e\,^3\Pi$ state. The radiative deexcitation rate of the upper electronic state is 6.2×10^7 sec^{-1}; the corresponding two-body quenching rate by collisions with neutral helium atoms at 295°K is 7.1×10^{-11} cm^{3}sec^{-1}. The total two-body rotational relaxation rate of the $J=6$ level by collisions with neutrals is 5.8×10^{-10} cm^{3}sec^{-1}. While collisions with $\Delta J=\pm1$ account for more than 60% of total rotational transfer, it is necessary to include a substantial probability of multiquantum rotational transitions in order to explain the observed results.

I. INTRODUCTION

The most prominent feature of the visible molecular helium spectrum is probably the band near 4650 Å,[1-3] which corresponds to the $v=0$ transition from the $He_2(e\,^3\Pi_g)$ state to the $He_2(a\,^3\Sigma_u^+)$ metastable state. Individual lines are easily resolved within this band; it comprises three branches labeled P, Q, and R (Fig. 1); they correspond to transitions with $\Delta J=+1$, 0, and -1, respectively, where J is the rotational quantum number.[4] Since the mass-4 isotope of helium has zero nuclear spin, even labeled lines are missing.[2]

We have measured the radiative transition probability, the corresponding two-body quenching rate by collisions with neutral helium atoms, and the effective rate of rotational relaxation through collisions of the $J=1-8$ rotational sublevels of $He_2(e\,^3\Pi_g)$ in a well-diagnosed room-temperature afterglow plasma. With a short-pulse tunable dye laser we have selectively pumped the $R(5)$ $[(J=5)\rightarrow(J=6)]$ transition of the e-a band. The relative populations of the $J=1$ to $J=8$ sublevels are then followed on a nanosecond time scale through their fluorescent light intensities.

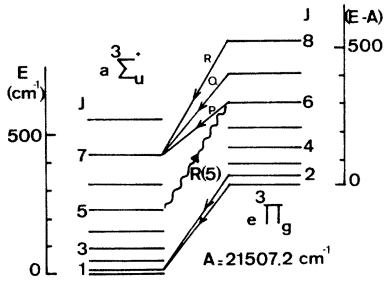

FIG. 1. Rotational energy levels of the a and e states of $He_2(v=0)$ involved in this experiment; the wavy line corresponds to the $R(5)$ component used for optical pumping.

II. EXPERIMENTAL SYSTEM

Helium molecules in the $a\,^3\Sigma_u^+$ metastable states are readily formed under quasiequilibrium conditions in the stationary afterglow of an ultrapure helium plasma at pressures of a few Torr and higher.[5] Molecular metastable populations in excess of 10^{10} cm^{-3} are routinely maintained for several hundreds of microseconds after cessation of the active discharge.

We have used a standard ultra-high-purity helium cell[6] of 0.8 cm inside diameter and 38 cm total length fitted with tilted entrance and exit windows and centered inside a standard X-band waveguide (Fig. 2). No impurity lines were observed after prolonged bakeout of the cell and cataphoretic cleaning of the helium gas. A plasma was created every 120 msec by a high-voltage (4.5 kV), low-current (100 mA) pulse. Gas heating was negligi-

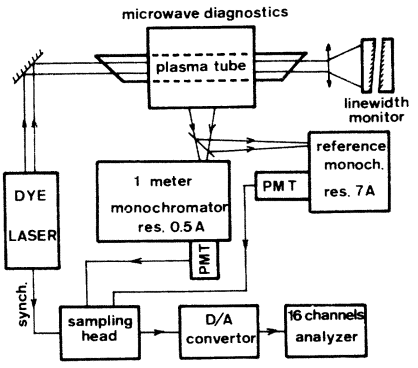

FIG. 2. Simplified schematic diagram of the experimental system (not to scale).

ble and the neutral gas temperature was between 295 and 300°K.

Electron density and temperature were routinely measured by microwave diagnostics[5] as a function of time in the afterglow. The electron temperature could be changed at a selected time by a medium-power (≤300 mW) pulsed microwave heating field at X-band frequencies. As will be seen later, this is particularly useful for distinguishing electronic and neutral deexcitation phenomena.

The flowing dye laser and its nitrogen pump laser are commercial models (SOPRA). When using an ethanol solution of 7-diethylamino-4-methylcoumarin, the laser is tunable over most of the $He_2(a\text{-}e)$ rotational system (Fig. 1). It delivers more than 3×10^{13} photons per 3.5-nsec (full width at half-maximum) pulse. After passing through a set of lenses and diaphragms, the beam has a typical diameter of 1 mm with a divergence angle less than 2 mrad. The spectral width at half-maximum was of the order of 0.1 Å. The laser repetition period was 60 msec, i.e., one-half of the plasma repetition period.

Fluorescence light was observed at 90° to the laser beam (Fig. 2) through a 10-cm-long, 0.15-cm-wide longitudinal slot centered on the larger side of the waveguide enclosing the plasma tube. Before entering the cell, the beam was expanded to a diameter of 4 mm so that one-half of the radial dimension of the cell was illuminated. Light was analyzed with a 1-m Czerny-Turner monochromator equipped with a 1180 grooves/mm holographic grating. Slits were set to give a resolution of about 0.5 Å. Light intensities were measured with an RCA 4818 photomultiplier (PM) tube; its measured anode pulse rise time was 1.6 nsec. Anode connections were carefully terminated to avoid reflections and ringing. The wavelength difference between the laser light and the detected fluorescence light was always greater than 5 Å in order to minimize stray light rejection problems; owing to the high quality of the holographic grating, the remaining stray light level was very low and was easily made negligible by synchronous detection.

The linearity range of the PM tube under transient conditions[7] was ascertained by illuminating its photosensitive surface with the laser light after variable, calibrated attenuation. Fluorescent light intensities were then kept at least two orders of magnitude below the saturation level.

To avoid photon pileup problems near maximum fluorescence light intensity, the photomultiplier was used in an analogic mode, and its output amplitude was converted into digital form with a 1-nsec time resolution. The corresponding data were processed on-line after each laser shot by a 16-channel data acquisition system. The time between channels was nominally 1 nsec, with random deviations less than 50 psec. One channel was used to record the time-integrated fluorescence light intensity on the $Q(1)$ to $Q(7)$ lines (4649 to 4655 Å) measured through an auxiliary low-resolution monochromator. As this intensity was found to be proportional under constant experimental conditions to the laser power available on the width of the $R(5)$ line, convenient normalization of the fluorescence signals to the available laser power was made possible, as was, at the same time, constant monitoring of the laser output power.

The fringe pattern of a plane Fabry-Perot interferometer illuminated by a small fraction of the laser beam was also continually scanned with a television camera-monitor system to provide a continuous check of the laser linewidth and stability. The short-term frequency stability of the dye laser system was excellent, and periodic fine adjustments of the dye laser head were sufficient to maintain the reference signal near its nominal value. Fluorescence light intensities were usually very low and long integration periods were necessary; they were made possible by the excellent stability of the laser system.

III. EXPERIMENTAL RESULTS

A. Excited-states populations

We first evaluated without laser perturbation the relative populations of the $He_2(e\,^3\Pi_g)$ rotational sublevels by measuring light intensities on the lines of the P, Q, and R branches of the corresponding e-a electronic transitions from $J=2$ to $J=13$. Assuming Hönl-London rotational line strengths to be nearly valid in this case,[4] we always found Boltzmann distributions among rotational sublevels at temperatures ranging from 500 to 700°K, i.e., substantially above gas temperature (295 to 300°K). Typical results are shown in Fig. 3, where we have plotted in arbitrary units the ratio of the measured intensities to the line strength as a function of the rotational energy. As reported previously,[3] there was no marked dependence on electron density or temperature or on gas pressure.

The laser was then turned on and tuned to the $R(5)$ line, and we followed the time evolution of the fluorescence light intensity on selected transitions originating from the $J=1$ to $J=8$ levels of the e state.

Typical time evolutions of reduced populations n_J/g_J, where $g_J=2J+1$ is the rotational level degeneracy, are shown for $J=2$, 6, and 7 in Fig. 4

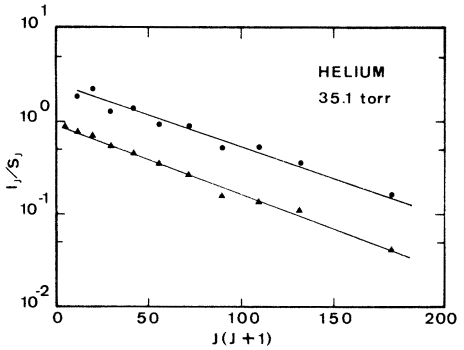

FIG. 3. Rotational line intensities I_J divided by the corresponding Hönl-London factors S_J, plotted vs rotational energy. ●: data obtained at $n_e = 2.1 \times 10^{11}$ cm^{-3}, $T_e = 650$ °K; ▲: data obtained at $n_e = 1.5 \times 10^{11}$ cm^{-3}, $T_e = 400$ °K. In both cases, the rotational temperature is close to 610 °K.

for a gas pressure of 35.1 Torr and in Fig. 5 for a pressure of 16.5 Torr. (Populations of other rotational levels up to $J = 8$ have been measured but are omitted for clarity.) In both cases the $J = 6$ level is seen to be directly populated during the laser pulse; the other rotational levels are then indirectly populated through inelastic collisions which redistribute rotational energy. A Boltzmann distribution is found to be established

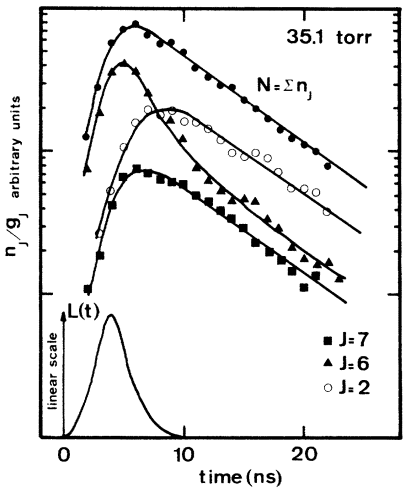

FIG. 4. Time evolution of reduced populations n_J/g_J for three selected rotational levels at 35.1 Torr. Populations of other rotational levels have been measured up to $J = 8$ but are omitted for clarity. The data points result from a three-point binomial smoothing of experimental data and the curves are the result of the best fit through Eq. (1) with the rates given in Sec. III. The total population $N = \sum_J n_J$ of the $e^3\Pi_g$ state decays exponentially with a rate constant ν_{el} after the end of the laser pulse; the shape of the laser pulse is shown at the bottom of the figure.

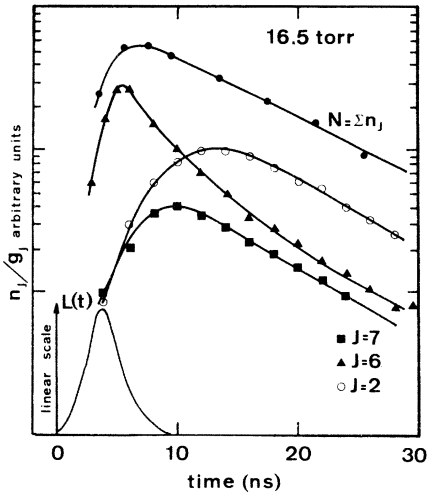

FIG. 5. Same as Fig. 4, but at a pressure of 16.5 Torr.

among rotational sublevels at later times ($t \gtrsim 15$ nsec at 35.1 Torr and $T \gtrsim 30$ nsec at 16.5 Torr). The corresponding characteristic temperature is equal to the gas temperature, within the error bars; this contrasts with the unperturbed case, where the equilibrium temperature was about twice as large. This points to a strong rotational energy-source term in the helium afterglow, possibly in relation to the electronic recombination of the He_2^+ ion, and to simultaneous associative transfers from the He* to the He_2* systems.[8,9] The fact that the rotational populations relax with the same time constants at later times while being in thermodynamic equilibrium among themselves indicates that radiative decay or collisional quenching rates of the electronic excitation are independent of rotational quantum number. The rotational sublevel populations n_J as a function of the time should then be solution of the system of coupled differential equations

$$\frac{dn_J}{dt} = \nu_{rot} \sum_K (P_{JK} n_K - P_{KJ} n_J) - \nu_{el} n_J + \delta_{JM} L(t) , \tag{1}$$

where the relaxation rate of the electronic excitation ν_{el} is independent of the rotational quantum number J. $L(t)$ is the laser source term (see Figs. 4 and 5) and the Kronecker symbol δ_{JM} indicates that direct population occurs only in the M sublevel (in this case, $M = 6$). $\nu_{rot} P_{JK}$ is the $K \to J$ rotational transfer rate; the dimensionless partition coefficient P_{JK} may be *a priori* arbitrarily chosen for $J < K$, but microreversibility implies

$$P_{JK}(J > K) = P_{KJ}(g_J/g_K) \exp[-(E_J - E_K)/kT] , \tag{2}$$

where T is the temperature of the collisional re-

laxation partner and k is Boltzmann's constant. The rotational energy is $E_J = J(J+1)B$, where $B = 7.284\ \text{cm}^{-1}$ for $^4\text{He}_2(e\,^3\Pi_g)$.[3]

B. Decay of the electronic excitation

Since energy redistribution among rotational sublevels does not affect the total number $N = \sum_J n_J$ of molecules in the $e\,^3\Pi_g$ state, it is readily seen from Eq. (1) that

$$\sum_J \frac{dn_J}{dt} \equiv \frac{dN}{dt} = -\nu_{el} N + L(t)\,. \tag{3}$$

Typical time evolutions of $N(t)$ are shown at the top of Figs. 4 and 5; they are in detailed agreement with Eq. (3), $L(t)$ being proportional to the independently measured laser pulse shape and intensity. This indicates that the pumping transition is not saturated under our experimental conditions and that the role of stimulated emission is negligible. This is further confirmed by the observation that a fivefold attenuation of laser intensity does not significantly affect the shape of the $N(t)$ curve.

The relaxation rate ν_{el} of the electronic excitation is easily deduced from plots of $N(t)$ such as those shown in Figs. 4 and 5. Its general form may be expected[10] to be

$$\nu_{el} = A_R + k_0[\text{He}] + k_e n_e\,, \tag{4}$$

where A_R is the radiative rate and where k_0 and k_e are the rates for deexcitation by collisions with neutrals of density [He] and with electrons of density n_e, respectively. Within error bars, ν_{el} was found to be independent of electron density and temperature over the range covered with this experimental system (density from 5×10^{10} to 10^{11} cm^{-3} and temperature raised by microwave heating from 300 to 1700 °K). It should, however, be noted that analogous measurements by selective excitation spectroscopy on the *atomic* helium triplet system[11] show atomic collisional deexcitation rates to be electron-temperature and -density dependent over a similar range. We may conclude that between 300 and 1700 °K $k_e(e\,^3\Pi_g) \leq 2\times10^{-5}$ $\text{cm}^3\,\text{sec}^{-1}$.

On the other hand, the relaxation rate ν_{el} was found, within error bars, to vary linearly with helium pressure (Fig. 6). Measurement of the slope of the least-squares line and of its zero-pressure intercept yields a radiative deexcitation rate $A_R = (6.2\pm0.5)\times10^7\ \text{sec}^{-1}$ and a rate of two-body quenching by collisions with neutral helium atoms at 295 °K of $k_0 = (7.1\pm0.6)\times10^{-11}\ \text{cm}^3\,\text{sec}^{-1}$. The radiative lifetime of $\text{He}_2(e\,^3\Pi_g)$ (16 nsec) is thus substantially smaller than that of $\text{He}(3\,^3P)$, which was found to be 94 nsec by using a similar technique in the same experimental system,[11] in good agreement with accepted values. The radiative molecular lifetime corresponds to deexcitation through the two allowed radiative channels, $e\,^3\Pi_g \rightarrow a\,^3\Sigma_u^+$ and $e\,^3\Pi_g \rightarrow d\,^3\Sigma_u^+$ (Fig. 7). Since the branching ratio of these two channels could not be measured in this particular experiment, it offers no final indication on the oscillator strength to be used in absolute spectroscopic density measurements using the e-a transition in absorption[12] or in emission.[13]

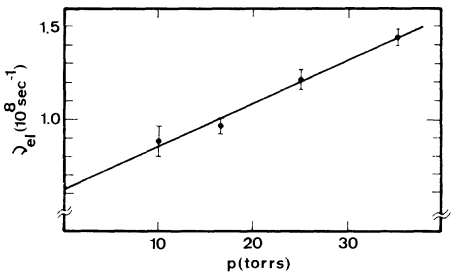

FIG. 6. Stern-Volmer plot of the relaxation frequency ν_{el} of the electronic excitation as a function of pressure.

The collisional quenching reaction may be written

$$\text{He}_2(e\,^3\Pi_g) + \text{He} \rightarrow \text{He}_2(X) + \text{He}\,, \tag{5}$$

where X denotes several electronically excited states of the molecule. The most likely candidates are the states $f\,^3\Sigma_u^+$, $f\,^3\Pi_u$, and $f\,^3\Delta_u$ (see Fig. 7), whose lowest rotational and vibrational levels

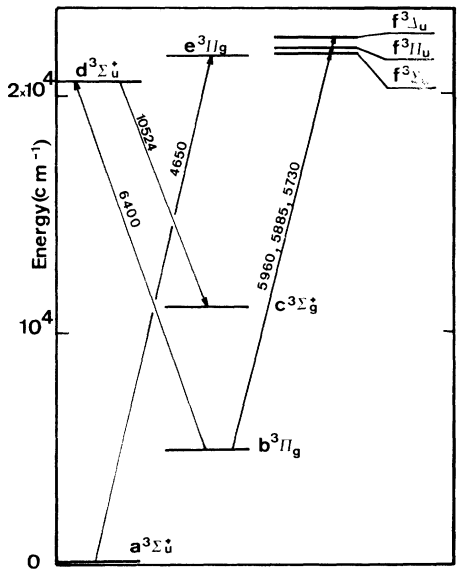

FIG. 7. Electronic energy levels at equilibrium internuclear separation of the triplet molecular states of He_2 involved in this experiment (transition wavelengths in Å).

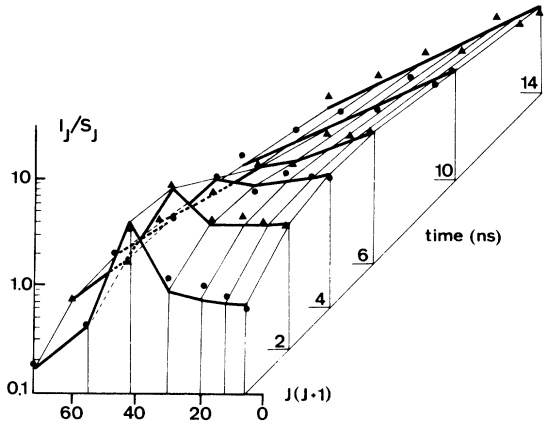

FIG. 8. Reduced rotational line intensities as a function of rotational energy and of time after peak laser power at 35.1 Torr. Dots and triangles are experimental data, and the lines represent the best fits through Eq. (1) with the rates given in Sec. III.

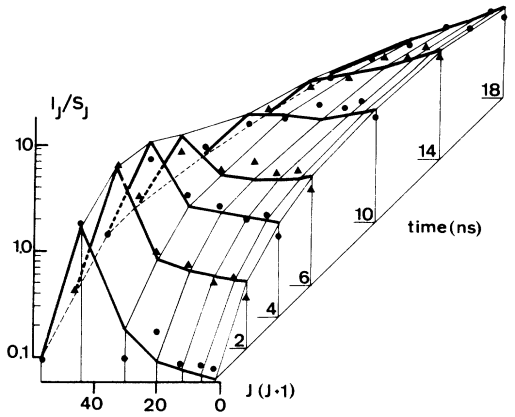

FIG. 9. Same as Fig. 8, but at a pressure of 16.5 Torr.

stand, respectively, at 41.6, 246.8, and 698.3 cm^{-1} above the $He_2(e\,^3\Pi_g, J=1, v=0)$ level. These states are optically connected to the $b\,^3\Pi_g$ state by the transitions around 5960, 5885, and 5730 Å, respectively. Fluorescent light induced by the pumping of the $He_2(e\,^3\Pi_g, J=6)$ level was observed around 5960 and 5730 Å, but emission at 5885 Å was masked by the strong atomic line at 5876 Å. The time-integrated light intensities at 5960 and 5730 Å, normalized to the time-integrated light intensity around 4650 Å, were found to be independent of electron density and temperature; this confirms that under our experimental conditions the free electrons of the plasma play a negligible role in the collisional transfer of electronic excitation from the $He_2(e\,^3\Pi_g)$ level to its nearest neighbors.

C. Rotational relaxation

We have studied transfer processes among rotational sublevels at 16.5 and 35.1 Torr (Figs. 4 and 5). A comparison of the behavior of the $J=6$ level (which is directly populated during the laser pulse) and of the $J=7$ level (which is populated by rotational transfer) shows immediately that the optical selection rule $\Delta J=\pm 2$ for homonuclear zero-spin molecules does not hold for collisional transfer under our experimental conditions.

Following Polanyi and Woodall,[14] we have compared our experimental results to the predictions of a model where the partition coefficient for downward transitions (i.e., $K>J$) has the form

$$P_{JK}=(g_J/g_K)\exp[-C(E_K-E_J)/kT], \qquad (6)$$

where C is an adjustable coefficient. The partition coefficient for upward transitions is deduced from (6) through the microreversibility relation (2). The temperature T of the heat bath was 295 °K. We found that our results were well fitted (see Figs. 8 and 9) by this model if we set $C=1$ to within 10% and if we put $\nu_{rot}=1.4\times10^8$ sec^{-1} at 16.5 Torr and 3.1×10^8 sec^{-1} at 35.1 Torr. The total rotational relaxation rate of the $J=6$ level is then $\nu_{rot}\sum_K P_{K6}=(1.9\pm0.2)\times10^7 p$ (sec^{-1}), where the pressure p is in Torr. This corresponds at 295 °K to a two-body rate of 5.8×10^{-10} $cm^3\,sec^{-1}$. Comparably large rotational transfer rates have been reported in other diatomic molecules.[15]

While collisions with $\Delta J=\pm1$ account for more than 60% of the total collisional transfer, as noted by Collins and Johnson,[16] consideration of Figs. 4 and 5 shows that collisions with a large rotational-quantum-number change play a significant role in the evolution of excited-states populations during and after the laser pulse; this feature, which is correctly taken into account in the model, is also in agreement with observations made in other diatomic molecules.[15,17]

ACKNOWLEDGMENTS

It is a pleasure to acknowledge several helpful discussions with Dr. L. Goldstein and Dr. J. Stevefelt as well as the highly efficient technical help of J.-P. Puissant. This work was supported by Direction des Recherches et Moyens d'Essai under Contract No. 74/418.

[1]W. H. J. Childs, Proc. R. Soc. A 118, 296 (1923).
[2]G. H. Dieke and E. S. Robinson, Phys. Rev. 80, 1 (1950).
[3]For a summary of the spectra and structure of excited states of He_2, see M. L. Ginter, in *Spectroscopic Data Relative to Diatomic Molecules*, edited by B. Rosen (Pergamon, Oxford, 1970), p. 193.
[4]G. Herzberg, *Spectra of Diatomic Molecules* (Van Nostrand, Princeton, 1950).
[5]J.-F. Delpech, J. Boulmer, and J. Stevefelt, in *Advances in Electronics and Electron Physics*, edited by L. Marton (Academic, New York, 1975), Vol. 39, p. 121.
[6]C. Sol, J. Boulmer, and J.-F. Delpech, Phys. Rev. A 7, 1023 (1973).
[7]P. F. Jones and A. R. Calloway, Rev. Sci. Instrum. 44, 1393 (1973).
[8]J. Boulmer, J. Stevefelt, and J.-F. Delpech, Phys. Rev. Lett. 33, 1248 (1974).
[9]A. B. Callear and R. E. M. Hedges, Trans. Faraday Soc. 66, 2921 (1970).
[10]H. F. Wellenstein and W. W. Robertson, J. Chem. Phys. 56, 1072 (1972).
[11]J.-P. Moy, J.-C. Gauthier, and J.-P. Geindre, in Proceedings of the Twelfth International Conference on Phenomena in Ionized Gases, Eindhoven, 1975, p. 16 (unpublished).
[12]L. C. Pitchford, K. N. Taylor, and C. B. Collins, J. Phys. B 8, 142 (1975).
[13]J. Stevefelt and J. Robben, Phys. Rev. A 5, 1502 (1972).
[14]J. C. Polanyi and K. B. Woodall, J. Chem. Phys 56, 1563 (1972).
[15]K. Bergmann and W. Demtröder, J. Phys. B 5, 2098 (1972).
[16]C. B. Collins and B. W. Johnson, J. Chem. Phys 57, 5317 (1972).
[17]W. H. Duewer, J. A. Coxon, and D. W. Setser, J. Chem. Phys. 56, 4355 (1972).